

## Research Article

**Induction of Osteogenesis After BMP-2 Injection in Rabbit Shoulders: A Novel Strategy for Managing Glenoid Bone Defect Associated with Anterior Shoulder Instability**Sang Yun Oh<sup>1</sup>, Young Hoon Jang<sup>4</sup>, Dong Mo Kang<sup>5</sup>, Jung Hoon Choi<sup>2</sup>, Jin-Young Chung<sup>3</sup> and Sae Hoon Kim<sup>1\*</sup><sup>1</sup>Department of Orthopedic Surgery, Seoul National University College of Medicine, Seoul National University Hospital, Korea<sup>2</sup>Department of Veterinary Anatomy and Institute of Veterinary Science, College of Veterinary Medicine, Kangwon National University, Korea<sup>3</sup>Department of Veterinary Internal Medicine and Institute of Veterinary Science, College of Veterinary Medicine, Kangwon National University, Korea<sup>4</sup>Department of Orthopedic Surgery, Chungmu (CM) Hospital, Korea<sup>5</sup>Department of Orthopaedic Surgery, Chambaro Hospital, Seoul, Korea

## ARTICLE INFO

## Article history:

Received: 21 July, 2023

Accepted: 24 August, 2023

Published: 1 September, 2023

## Keywords:

*Bone morphogenic protein-2, glenoid defect, osseous bankart lesion, shoulder instability*

## ABSTRACT

**Background:** Bone morphogenic protein-2 (BMP-2) has been shown to promote bone formation. The purpose of this research was to determine if an injectable form of BMP-2 could induce bone formation in antero-inferior glenoid bone defects, which is a critical factor of anterior shoulder instability. The purpose of this study was to investigate bone formation in rabbit shoulders following BMP-2 injection into the anterior capsulolabral complex. We hypothesized that the amount of new bone would be greater in rabbit shoulders injected with BMP-2 than in those injected with normal saline. **Methods:** An experimental study was conducted on 40 shoulders of 20 mature rabbits. Twenty right shoulders were allocated to four groups according to injection dose (5 µg or 10 µg) and follow-up period after injection (4 or 8 weeks). Twenty left shoulders were injected with normal saline as controls. At 4 or 8 weeks after injection, all rabbits were sacrificed, and bone volumes, densities, and locations of bone formation were evaluated using micro-computed tomography (micro-CT). Histologic analysis was performed on all 40 shoulders. **Results:** Shoulders injected with BMP-2 showed significantly more bone formation than control shoulders in all treated groups ( $58.6 \pm 60.5 \text{ mm}^3$  vs.  $25.6 \pm 32.6 \text{ mm}^3$ ,  $p = 0.001$ ). Moreover, bone formation increased with dose and follow-up. Locations of bone formation were the lesser tuberosity, greater tuberosity, and anterior capsulolabral complex. Histologic analysis confirmed the micro-CT-detected bone formation by revealing the presence of activated osteocytes, abundant osteoblastic rimming, and woven bone matrix. **Conclusion:** The study confirms that BMP-2 injection into the anterior capsulolabral complex of rabbit shoulders promotes new bone formation in adjacent soft tissue areas. **Study Design:** Controlled laboratory study.

© 2023 Sae Hoon Kim. Published by World Journal of Surgery

**1. Introduction**

‘A golf ball on a tee’ refers to the bony conformation between the humeral head and the glenoid that provides static stability [1]. Dynamic factors such as the rotator cuffs serve as the gravity on the “ball on the tee”, by generating compressive force to secure glenohumeral stability. The congruent bony structure acts as a fulcrum that counteracts and balances the force, thus the bony conformation has been increasingly emphasized by many researchers [2, 3]. Recently, a relatively small glenoid defect, as little as 17.3 % of its diameter, was shown to critically disrupt the joint stability [4]. Therefore, many strategies have been

reported to resolve shoulder joint instability by recovering the critical defect of “the tee” [5].

Initially, surgical strategies aimed to augment the glenoid defect using bone grafts as a bumper [5]. Stratified procedures include coracoid process transfer with conjoined tendon and coracoacromial ligament, known as Latarjet procedure, or attachment of autologous iliac bone graft, presented as Eden-Hybinnette procedure and Bristow procedure [6-8]. Although these procedures are accepted as rational options for large glenoid defects, complications such as loss of external rotation and early osteoarthritis have been reported by several authors. These may result from adhesive scarring due to invasive nature of the procedures,

\*Correspondence to: Sae Hoon Kim, M.D., Ph.D., Department of Orthopaedic Surgery, Seoul National University Hospital, 101 Daehak-ro, Jongno-gu, 110-744, Seoul, Korea; E mail: [drjacobkim@gmail.com](mailto:drjacobkim@gmail.com)

and altered mechanical conditions from non-anatomical reconstruction [5].

On the other hand, Bone morphogenetic protein-2 (BMP-2) is known to be one of the most potent factors to induce bone formation [9]. It has been used to induce bone union in the spine fusion site or long bone fracture site, and to promote bone-tendon healing in rotator cuff tears by inducing osteogenesis [10]. Meanwhile, heterotopic ossification (HO), osteogenesis outside of the site of interest, is a well-recognized side effect of BMP-2 [9]. Despite the potential for HO to address glenoid defects causing anterior glenohumeral instability, no studies have investigated its possibility.

To primarily address this issue, we proceeded a preliminary experiment using rabbit shoulders. Our hypothesis was that the amount of new bone would be higher in a rabbit shoulder injected with BMP-2 than in that injected with normal saline.

## 2. Materials and Methods

### 2.1. Study Design

All experimental procedures were approved by the experimental animal committee of the clinical research institute of the authors' affiliated institution, and the experiments were conducted in accordance with the institution's guidelines for the care and the use of laboratory animals. This was a controlled laboratory study involving animals. Power analysis indicated that sample size of five for each group was required to detect a significant difference in the volume of new bone (mean

difference, 10 %; standard deviation, 5 %; alpha-error, 0.05; beta-error, 0.2; drop-out rate, 20%), based on previous studies [10, 11].

We randomly allocated 20 healthy New Zealand white male rabbits (average age, 24 weeks old; weight, 3.5 - 4.0 kg) into four groups (5 rabbits per group) with respect to dose of the injected BMP-2 (5  $\mu$ g or 10  $\mu$ g), and the follow-up period after the injection (4 or 8 weeks): group A, 5  $\mu$ g, 4 weeks; group B, 10  $\mu$ g, 4 weeks; group C, 5  $\mu$ g, 8 weeks; group D, 10  $\mu$ g, 8 weeks. Right shoulders of each group were injected with BMP-2 solution, while left shoulders were injected with the same amount of normal saline as negative controls.

### 2.2. Operation Technique and BMP-2 Injection

All surgical procedures were performed by the same surgeon (corresponding author). Anesthesia was induced with an intramuscular injection of 15 mg/kg zolazepam (Zoletil; Virbac S.A., Carros, France) and 5 mg/kg xylazine hydrochloride (Rompun; Bayer HealthCare, Leverkusen, Germany). Prior to the procedures, 30 mg/kg prophylactic cefazolin (Cefamezin; Dong-A Pharm, Seoul, Korea) was administered. After thorough shaving and skin preparation, a sterile drape was applied. For each right shoulder, an anterior longitudinal incision was made, and the deltopectoral interval was identified and split. The subscapularis tendon was identified and partially split horizontally to expose the capsule and anterior labrum (Figure 1). BMP-2 solutions were obtained by mixing 5  $\mu$ g or 10  $\mu$ g of recombinant human BMP-2 powder (Novosis; CGBio, Gyeonggi-do, Korea) with 1 mL sterile normal saline. 1 mL of the BMP-2 solution was divided into three injections, targeting the anterior labrum and anterior capsule of the anterior capsulolabral complex.

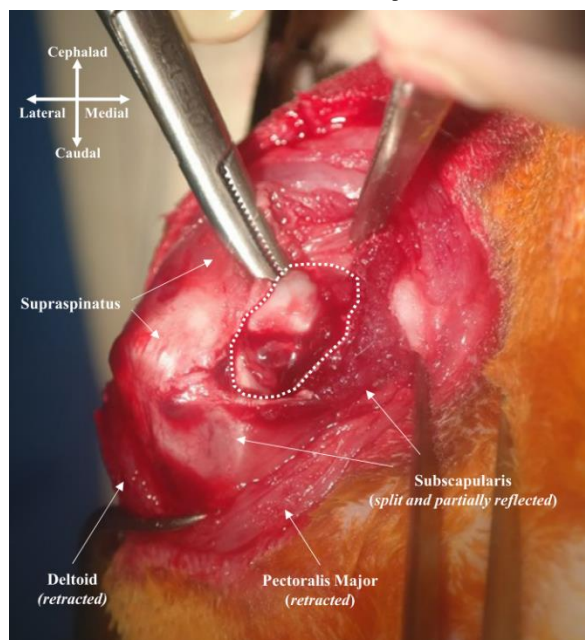


**FIGURE 1:** Exposure of anterior capsulolabral complex.

This image shows anterior view of right rabbit shoulder. Deltopectoral interval was split and the subscapularis was partially split longitudinally to tendon direction and reflected. The white dotted area represents anterior capsulolabral complex, where BMP-2 solution was injected.

After the injection, the fascia and subcutaneous tissues were sutured using interrupted 3-0 vicryl sutures (Ethicon, Somerville, NJ, USA), and

the skin was sutured using interrupted 3-0 nylon sutures (Ethicon, Somerville, NJ, USA). The same surgical procedures, with normal saline

instead of BMP-2 solution, were repeated for the left shoulders. On the day of the operation and the first three postoperative days, the rabbits were given a subcutaneous injection of 0.2 mg/kg meloxicam (Metacam; Boehringer Ingelheim, Ingelheim am Rhein, Germany) for analgesia. An intramuscular injection of 30 mg/kg cefazolin (Cefamezin; Dong-A Pharm, Seoul, Korea) was also administered once a day as a prophylactic. The rabbits were not immobilized postoperatively, with their limbs free to move in the respective cages.

### 2.3. Radiologic Evaluation

At 4 weeks postoperatively, rabbits in group A and B were euthanized with carbon dioxide, while rabbits in group C and D were euthanized at 8 weeks postoperatively. The entire shoulder joint, including lateral half

of the scapula and proximal one third of the humerus, along with all the soft tissue, was harvested from each rabbit. Micro-CT scanning was then performed on all specimens using micro-CT system (NFR-Polaris-G90; NanoFocusRay, Iksan, Korea) operated at a voltage of 65 kV and a current of 0.12 mA with a 0.1 mm thickness. To obtain 3D volume measurements of HO, micro-CT images were reconstructed using 3D slicer software version 4.10.2 (NIH-funded, open source) [12]. 3D bone models of bilateral shoulders were obtained semi-automatically with a threshold setting for bone density. HO was defined by subtracting a mirror model of the contralateral shoulder from the model of the ipsilateral shoulder (Figure 2). The volume and bone density of HO were measured using the same software for qualitative and quantitative measurement, respectively.

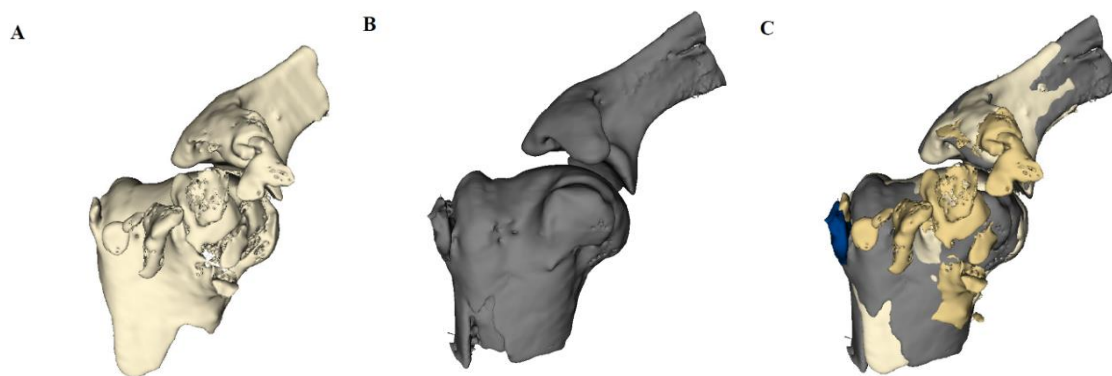


**FIGURE 2:** Defining heterotopic ossification (HO) using 3D model reconstructed from micro-computed tomography (micro-CT) images.

**A)** This is a 3D model that was reconstructed from micro-CT images of right shoulder in group D (specimen number 8R) after it was injected with bone morphogenic protein-2 (BMP-2). **B)** This is a mirror-image of the 3D model of the left shoulder of the same rabbit (specimen number 8L), which was injected with normal saline. **C)** Subtracting the mirror-image from the 3D model of interest makes it possible to define HO. The golden masses represent HO on BMP-2 side, while dark blue mass represents HO on the control side of specimen number 8.

### 2.4. Histologic Evaluation

Immediately after obtaining micro-CT images, the specimens were fixed in neutral-buffered 10% formalin (pH 7.4) and decalcified. Paraffin blocks were made in the affected region, and serial sections were cut and stained with hematoxylin and eosin to evaluate HO histologically. To minimize any observer bias, all analyses were performed in a blinded fashion with respect to the group assignment.

### 2.5. Statistical Analysis

The statistical analysis was conducted using SPSS version 25.0 (IBM SPSS Statistics, Chicago, IL, USA). All p-values reported were two-sided, with p-values < 0.05 as statistical significance. Descriptive statistics were presented as mean  $\pm$  standard deviation. The normality of the distribution was analyzed using Kolmogorov-Smirnov test. Paired t-test was used to compare the bone density between HO and the native bone. Wilcoxon test was performed to compare the volume of HO on BMP-2 side with that on the control side. Pearson's correlation coefficient (PCC) was calculated to determine the nature of correlation

between the volume of HO on BMP-2 side and that on the control side. The sample size was calculated using G\*power version 3.1.9.4 software.

## 3. Results

### 3.1. Radiologic Analysis

All twenty shoulders on BMP-2 side presented HO on micro-CT scan. HO had a uniform morphologic feature, as thinner cortex and less organized trabecular pattern in the medulla with relatively lower attenuation than the native bone. (Figure 4B, Figure 5B). While some HO was attached to the native bone, it was well-demarcated from the native bone. HO was distributed on the anterior side of the shoulder, mostly located in the lesser tuberosity (LT), greater tuberosity (GT) and anterior capsulolabral complex. Besides, some HO was detected in the deltoid muscle (Table 1).

The mean volume of HO on BMP-2 side was  $58.8 \pm 60.5$  mm<sup>3</sup> with ranges from 5.2 mm<sup>3</sup> to 227.1 mm<sup>3</sup>. With respect to the injection dose (5  $\mu$ g vs. 10  $\mu$ g), the mean volume of HO was greater when a higher dose was injected in both 4-week groups (Group A vs. B) and 8-week groups

(Group C vs. D). As for the follow-up period (4 weeks vs. 8 weeks), longer follow-up showed a higher volume of HO, regardless of the dose of HO injection (Table 2). The bone density of HO on BMP-2 side of all pairs of 20 shoulders was lower than that of native bone (1611 HU vs.

2284 HU,  $p < 0.001$ ). While there was no difference in bone density on BMP-2 side between the injection dose, a significant difference was observed where the 8-week groups (Group C and D) exhibited higher bone density than the 4-week groups (Group A and B) (Table 3).

**TABLE 1:** Location of heterotopic ossification.

Group	Dose (µg)	Follow-up (weeks)	LT	GT	Anterior glenoid /Anterior glenoid	Deltoid
A (n = 5)	5	4	3	3	4	3
B (n = 5)	10	4	4	3	1	1
C (n = 5)	5	8	4	2	2	3
D (n = 5)	10	8	5	2	2	1
<b>Total (n = 20)</b>			16	10	9	8

LT: The lesser trochanter of the humerus, GT: The greater trochanter of the humerus. Data represent number of specimen, otherwise unspecified.

**TABLE 2:** Volume of heterotopic ossification measured in micro-computed tomography.

Group	Dose (µg)	Follow-up (weeks)	Volume at BMP-2 side (mm <sup>3</sup> , α)	Volume at control side (mm <sup>3</sup> , β)	Δ Volume (mm <sup>3</sup> , α-β)
A (n = 5)	5	4	26.7 ± 29.2	8.8 ± 14.8	16.8 ± 15.7
B (n = 5)	10	4	46.6 ± 48.2	29.0 ± 44.9	17.6 ± 12.7
C (n = 5)	5	8	76 ± 55.7	29.9 ± 38.5	52.1 ± 41.3
D (n = 5)	10	8	86.1 ± 91.4	35.5 ± 30.4	50.5 ± 62.1

BMP-2: Bone morphogenic protein-2. Data represent mean ± standard deviation.

**TABLE 3:** Bone density of heterotrophic ossification determined by mean Hounsfield unit in micro-computed tomography.

Group	Dose (µg)	Follow-up (weeks)	Bone density at BMP-2 side (HU)	Bone density at control side (HU)
A (n = 5, 3)*	5	4	1528 ± 140	1652 ± 43
B (n = 5, 4)*	10	4	1509 ± 115	1566 ± 143
C (n = 5, 3)	5	8	1708 ± 207	1643 ± 69
D (n = 5, 5)	10	8	1700 ± 166	1549 ± 202

BMP-2: Bone morphogenic protein-2. Data represent mean ± standard deviation, otherwise unspecified.

\*Numbers in parenthesis refer to number of specimen of each group. The former refers to number of specimen of BMP-2 side, the latter refers to that of control side. Note that 3 of 5 shoulders in group A showed HO at control side, and that 4 of 5 shoulder in group B did.

Shoulders on the control side, injected with normal saline, also presented HO. Sixteen out of twenty shoulder on control side showed HO in micro-CT images. The mean volume of HO in the control side was 25.6 mm<sup>3</sup> ± 32.6 mm<sup>3</sup> with ranges from 0 mm<sup>3</sup> to 108.4 mm<sup>3</sup>. It was significantly lower than that on BMP-2 side ( $p = 0.001$ ). The morphologic

characteristic of HO on the control side showed similar features to that on BMP-2 side (Figure 3). Strong correlation was observed between HO volume on BMP-2 side and that on the control side ( $PCC = 0.837$ ,  $p < 0.001$ ). The bone density of HO on the control side was lower than that of native bone (1593 vs. 2339,  $p < 0.001$ ), however, it showed no

consistent trend regarding dose or follow-up period. We also assessed the effect of BMP-2 on HO by calculating the difference in volume,  $\Delta$  volume, by subtracting volume on the control side from that on BMP-2

side. Mean  $\Delta$  volume of HO was higher with longer follow-up, while a less difference of  $\Delta$  volume of HO with respect to the dose was observed (Table 2).

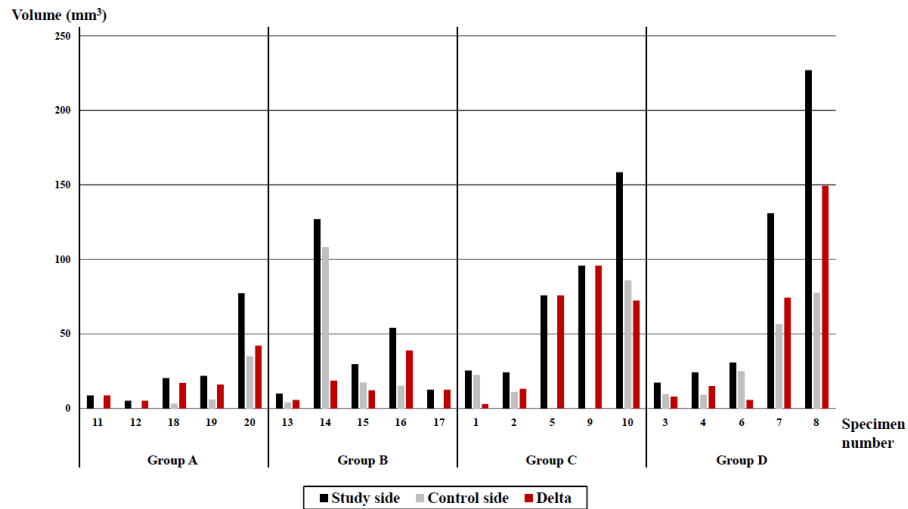


FIGURE 3: Volume of heterotopic ossification determined by micro-computed tomography.

### 3.2. Histologic Analysis

As demonstrated in (Figures 4 & 5), histologic analysis revealed that HO showed histologic feature of osteogenesis, including activated osteocytes, abundant osteoblastic rimming and woven bone matrix.

Some samples showed a mixture of unorganized and chondroid matrix, suggesting ongoing enchondral ossification (Figures 4E-4F). HO of 4-week groups had more woven bones, while that of 8-week groups had more lamellar bones.

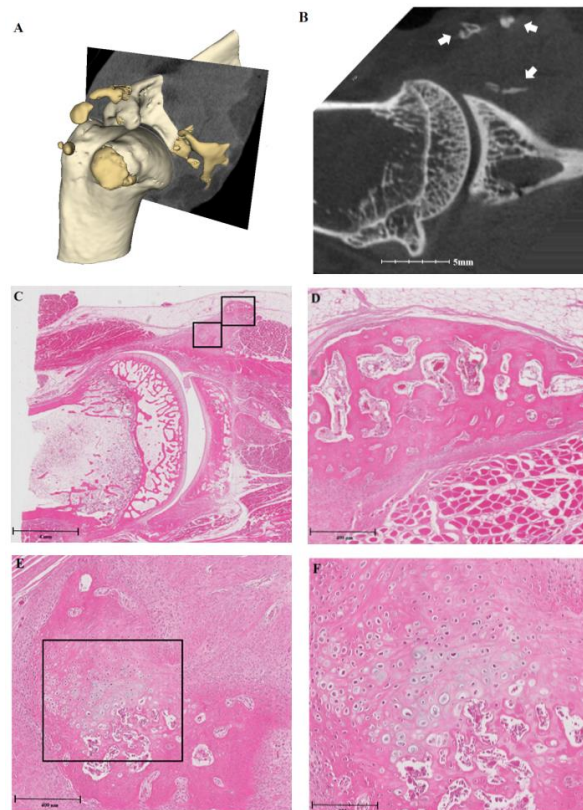
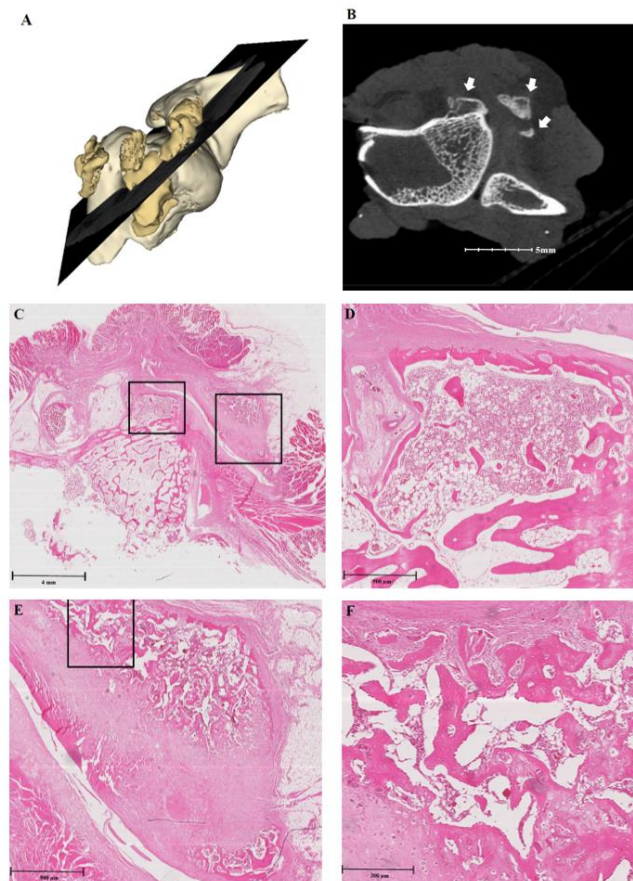


FIGURE 4: Histologic analysis of the right side of specimen number 14 in group A, which was followed up for 4 weeks.

A) This shows a 3D model of the specimen, with pale yellowish masses representing native bone, and golden masses representing heterotopic ossification (HO). B) Micro-computed tomography (micro-CT) image shows HO indicated by white arrows. C) Histologic section, stained with hematoxylin and eosin,

shows the same location as the micro-CT image. Black squares indicate HO and are magnified. **D**) Magnification of the right upper square in Figure 4C shows the histologic features of new bone formation, with activated osteocytes, abundant osteoblastic rimming and woven bone matrix. **E & F**) Second-order magnification of the left lower square in Figure 4C shows a mixture of unorganized and chondroid matrix, suggesting ongoing enchondral ossification.



**FIGURE 5:** Histologic analysis of the right side of specimen number 8 in group D, which was followed up for 8 weeks.

**A)** This shows a 3D model of the specimen, with pale yellowish masses representing native bone, and golden masses representing heterotopic ossification (HO). **B)** Micro-computed tomography (micro-CT) image shows HO indicated by white arrows. **C)** Histologic section, stained with hematoxylin and eosin, shows the same location as the micro-CT image. Black squares indicate HO and are magnified. **D)** Magnification of the left square in Figure 5C shows the features of woven bone, which are slightly more dense and have a more organized extracellular matrix, compared to images of Figure 2. **E & F)** Second-order magnification of the right square in Figure 5C shows a mixture of new bone with diverse mature states. Some portions show chondroid pattern, suggesting ongoing enchondral ossification.

#### 4. Discussion

This study demonstrated that the amount of HO was significantly higher in rabbit shoulders injected with BMP-2 compared to contralateral shoulders injected with normal saline. The sub-analysis revealed that the higher amount of HO was observed in the groups with a higher dose of BMP-2 or with a longer follow-up period. HO was mainly found at the LT, GT and anterior capsulolabral complex. HO showed morphologic features compatible with new bone in radiologic and histologic evaluations. Radiologically, HO detected by micro-CT showed a thin cortex and a less organized medulla with lower bone density than the native bone. Histologically, HO showed activated osteocytes, abundant osteoblastic rimming and a woven bone matrix. These features were more prominent in 8-week groups than in 4-week groups. Therefore, it is strongly suggested that local injection of BMP-2 to the anterior capsulolabral complex of rabbit shoulders promotes osteogenesis in the adjacent soft tissue area.

It was notable that HO was also observed on the control side, but the amount was significantly lower compared to BMP-2 side. The amount of HO on the control side was highly correlated with the amount on BMP-2 side. Two possible explanation could be suggested. One is that the sham surgical procedure, including dissection and needling, might cause HO on the control side as a surgical trauma [13]. With this perspective, the high correlation of HO volume between both sides might reflect individual susceptibility of each rabbit for factors causing HO, i.e. BMP-2 signal or surgical trauma. The other explanation of HO suggests remote effect of BMP-2. This could be supported by the fact that HO volume on the control side differed between group A and B or between group C and D, to which the same amount of normal saline was injected. The only difference between them was the dose on BMP-2 side. Further investigation is warranted to prove this effect of BMP-2.

The majority of new bones were formed at locations other than anterior capsulolabral complex, most frequently at the LT and GT. Leakage of

BMP-2 solution outside the injected area might cause HO, one of the most recognized complications of BMP-2 [9]. We reviewed that the volume of 1 mL was too large for small structures of rabbit shoulders, which might cause leakage. Therefore, further studies are needed to apply an appropriate carrier, such as collagen gel or sponge, fibrin gel, and beta-tricalcium phosphate, to secure the efficacy of BMP-2 and to prevent unintended ossification [14, 15]. Discovered in 1965 and first approved by the food and drug administration in the United States in 2002, BMP-2 has been widely used as a protein-based bone graft replacement [9, 16]. An epidemiological study found a 4-fold increase in annual number of procedures utilizing BMP-2 between 2003 and 2007, 85% of which were “off-label” use beside of approval for spine fusion or fracture union [17]. Considering this, BMP-2 can be a possible candidate for managing glenoid defects associated with anterior shoulder instability.

Recently, small bone fragments retained in osseous Bankart lesion gained attention after some researchers reported successful outcomes by incorporating them into the Bankart repair [20, 21]. Although previously ignored or removed during the repair [2, 22], several researchers found the evidence that the reduction and incorporation of small fragments with the repair may act as a core of glenoid reconstruction [23, 24]. In this perspective, it is important to restore glenoid size up to certain critical value, but not in the sense of “the more, the better” [4, 25]. Any harmful effects of invasive non-anatomical bone grafting should be avoided, particularly in cases of small bone defects. In this study, the BMP-2 injection promoted osteogenesis within the defect and anterior capsulolabral complex. Therefore, BMP-2 can be utilized as another core of non-invasive glenoid reconstruction for anterior shoulder instability.

This study has several limitations. Firstly, an optimal dose of BMP-2 has not been established on various administration sites for different animal models. The dose in this study was sufficient to confirm the osteogenic effect on glenoid defect, however, the volume might be excessive to prevent HO in untargeted areas. In addition, the 8-week experiment duration may be insufficient, as the shoulders in 8-week groups showed histological evidence of ongoing new bone formation. Compared with previous studies regarding osteoinduction of BMP-2 in rabbit models between 4-8 weeks [26-28], the exact chronology of ossification associated with BMP-2 is needed to be evaluated.

Lastly, additional research is required to establish a strategy for confining the effect of BMP-2 to intended area with contact to native glenoid. Nevertheless, ossification without contact to native glenoid could potentially provide stability to the glenohumeral joint, as Park *et al.* reported successful outcomes with fibrous union between the glenoid and bony fragment [24].

In conclusion, this study confirmed that BMP-2 injection to anterior capsulolabral complex of rabbit shoulders promotes osteogenesis in the adjacent soft tissue area. This phenomenon may potentially be used in treatment of glenoid bone defect associated with anterior shoulder instability.

#### Acknowledgements

None.

#### Funding

None.

#### Statement of Animal Rights

All experimental procedures were approved by the Experimental Animal Committee of the Clinical Research Institute of the authors’ affiliated institution, and the experiments were conducted in accordance with the institution’s guidelines for the care and the use of laboratory animals.

#### REFERENCES

- [1] Philipp Moroder, Lukas Ernstbrunner, Werner Pomwenger, et al. “Anterior shoulder instability is associated with an underlying deficiency of the bony glenoid concavity.” *Arthroscopy*, vol. 31, no. 7, pp. 1223-1231, 2015. View at: [Publisher Site](#) | [PubMed](#)
- [2] S S Burkhart, J F De Beer “Traumatic glenohumeral bone defects and their relationship to failure of arthroscopic Bankart repairs: significance of the inverted-pear glenoid and the humeral engaging Hill-Sachs lesion.” *Arthroscopy*, vol. 16, no. 7, pp. 677-694, 2000. View at: [Publisher Site](#) | [PubMed](#)
- [3] L Ernstbrunner, J D Werthel, T Hatta, et al. “Biomechanical analysis of the effect of congruence, depth and radius on the stability ratio of a simplistic ‘ball-and-socket’ joint model.” *Bone Joint Res*, vol. 5, no. 10:453-460, 2016. View at: [Publisher Site](#) | [PubMed](#)
- [4] Sang-Jin Shin, Yong Won Koh, Christopher Bui et al. “What is the critical value of glenoid bone loss at which soft tissue Bankart repair does not restore glenohumeral translation, restricts range of motion, and leads to abnormal humeral head position?” *Am J Sports Med*, vol. 44, no. 11, pp. 2784-2791, 2016. View at: [Publisher Site](#) | [PubMed](#)
- [5] Joseph R Lynch 1, Jeremiah M Clinton, Christopher B Dewing, et al. “Treatment of osseous defects associated with anterior shoulder instability.” *J Shoulder Elbow Surg*, vol. 18, no. 2, pp. 317-328, 2009. View at: [Publisher Site](#) | [PubMed](#)
- [6] A J HELFET “Coracoid transplantation for recurring dislocation of the shoulder.” *J Bone Joint Surg Br*, vol. 40, no. 2, pp. 198-202, 1958. View at: [Publisher Site](#) | [PubMed](#)
- [7] Rudolf Eden “Zur Operation der habituellen Schulterluxation unter Mitteilung eines neuen Verfahrens bei Abriss am inneren Pfannenrande.” *Deutsche Zeitschrift für Chirurgie*, vol. 144, pp. 269-280, 1918. View at: [Publisher Site](#)
- [8] Hybbinette S. “De la transplantation d’un fragment osseux pour remédier aux luxations récidivantes de l’épaule: Constatations et résultats opératoires.” *Acta Chir Scand*, vol. 71, no. 411-445, pp. 26, 1932.
- [9] Aaron W James, Gregory LaChaud, Jia Shen et al. “A review of the clinical side effects of bone morphogenetic protein-2.” *Tissue Eng Part B Rev*, vol. 22, no. 4, pp. 284-297, 2016. View at: [Publisher Site](#) | [PubMed](#)
- [10] Chih-Hwa Chen, Chih-Hsiang Chang, Kun-Chung Wang, et al. “Enhancement of rotator cuff tendon–bone healing with injectable periosteum progenitor cells-BMP-2 hydrogel *in vivo*.” *Knee Surg Sports Traumatol Arthrosc*, vol. 19, no. 9, pp. 1597-1607, 2011. View at: [Publisher Site](#) | [PubMed](#)

- [11] Hang Lin, Ying Tang, Thomas P Lozito, et al. "Efficient in vivo bone formation by BMP-2 engineered human mesenchymal stem cells encapsulated in a projection stereolithographically fabricated hydrogel scaffold." *Stem Cell Res Ther*, vol. 10, no. 1, pp. 254, 2019. View at: [Publisher Site](#) | [PubMed](#)
- [12] Andriy Fedorov, Reinhard Beichel, Jayashree Kalpathy Cramer, et al. "3D Slicer as an image computing platform for the Quantitative Imaging Network." *Magnetic resonance imaging*, vol. 30, no. 9, pp. 1323-1341, 2012. View at: [Publisher Site](#) | [PubMed](#)
- [13] William R Barfield, Robert E Holmes, Langdon A Hartscock "Heterotopic Ossification in Trauma." *Orthop Clin North Am*, vol. 48, no. 1, pp. 35-46, 2017. View at: [Publisher Site](#) | [PubMed](#)
- [14] Yoshihiro Hirakawa, Tomoya Manaka 2, Kumi Orita, et al. "The accelerated effect of recombinant human bone morphogenetic protein 2 delivered by  $\beta$ -tricalcium phosphate on tendon-to-bone repair process in rabbit models." *J Shoulder Elbow Surg*, vol. 27, no. 5, pp. 894-902, 2018. View at: [Publisher Site](#) | [PubMed](#)
- [15] Jae Gyoon Kim, Hak Jun Kim, Sung Eun Kim, et al. "Enhancement of tendon-bone healing with the use of bone morphogenetic protein-2 inserted into the suture anchor hole in a rabbit patellar tendon model." *Cytotherapy*, vol. 16, no. 6, pp. 857-867, 2014. View at: [Publisher Site](#) | [PubMed](#)
- [16] M R Urist "Bone: formation by autoinduction." *Science*, vol. 150, no. 3698, pp. 893-899, 1965. View at: [Publisher Site](#) | [PubMed](#)
- [17] Kevin L Ong, Marta L Villarraga, Edmund Lau, et al. "Off-label use of bone morphogenetic proteins in the United States using administrative data." *Spine (Phila Pa 1976)*, vol. 35, no. 19, pp. 1794-1800, 2010. View at: [Publisher Site](#) | [PubMed](#)
- [18] E Itoi, S B Lee, L J Berglund, et al. "The effect of a glenoid defect on antero-inferior stability of the shoulder after Bankart repair: a cadaveric study." *J Bone Joint Surg Am*, vol. 82, no. 1, pp. 35-46, 2000. View at: [Publisher Site](#) | [PubMed](#)
- [19] William H Montgomery Jr, Melvin Wahl, Carolyn Hettrich, et al. "Antero-inferior bone-grafting can restore stability in osseous glenoid defects." *J Bone Joint Surg Am*, vol. 87, no. 9, pp. 1972-1977, 2005. View at: [Publisher Site](#) | [PubMed](#)
- [20] Giuseppe Porcellini, Fabrizio Campi, Paolo Paladini "Arthroscopic approach to acute bony Bankart lesion." *Arthroscopy*, vol. 18, no. 7, pp. 764-769, 2002. View at: [Publisher Site](#) | [PubMed](#)
- [21] Hiroyuki Sugaya, Joji Moriishi, Izumi Kanisawa, et al. "Arthroscopic osseous Bankart repair for chronic recurrent traumatic anterior glenohumeral instability." *J Bone Joint Surg Am*, vol. 87, no. 8, pp. 1752-1760, 2005. View at: [Publisher Site](#) | [PubMed](#)
- [22] L U Bigliani, P M Newton, S P Steinmann, et al. "Glenoid rim lesions associated with recurrent anterior dislocation of the shoulder." *Am J Sports Med*, vol. 26, no. 1, pp. 41-45, 1998. View at: [Publisher Site](#) | [PubMed](#)
- [23] Young-Kyu Kim, Seung-Hyun Cho, Won-Su Son, et al. "Arthroscopic repair of small and medium-sized bony Bankart lesions." *Am J Sports Med*, vol. 42, no. 1, pp. 86-94, 2014. View at: [Publisher Site](#) | [PubMed](#)
- [24] Jin-Young Park, Seung-Jun Lee, Sang-Hoon Lhee, et al. "Follow-up computed tomography arthrographic evaluation of bony Bankart lesions after arthroscopic repair." *Arthroscopy*, vol. 28, no. 4, pp. 465-473, 2012. View at: [Publisher Site](#) | [PubMed](#)
- [25] Soichiro Kitayama, Hiroyuki Sugaya, Norimasa Takahashi et al. "Clinical Outcome and Glenoid Morphology After Arthroscopic Repair of Chronic Osseous Bankart Lesions: A Five to Eight-Year Follow-up Study." *J Bone Joint Surg Am*, vol. 97, no. 22, pp. 1833-1843, 2015. View at: [Publisher Site](#) | [PubMed](#)
- [26] Weibiao Huang, Brian Carlsen, Isabella Wulur, et al. "BMP-2 exerts differential effects on differentiation of rabbit bone marrow stromal cells grown in two-dimensional and three-dimensional systems and is required for in vitro bone formation in a PLGA scaffold." *Exp Cell Res*, vol. 299, no. 2, pp. 325-334, 2004. View at: [Publisher Site](#) | [PubMed](#)
- [27] K D Riew, N M Wright, S Cheng, et al. "Induction of bone formation using a recombinant adenoviral vector carrying the human BMP-2 gene in a rabbit spinal fusion model." *Calcif Tissue Int*, vol. 63, no. 4, pp. 357-360, 1998. View at: [Publisher Site](#) | [PubMed](#)
- [28] Louise L Southwood, David D Frisbie, Chris E Kawcak, et al. "Evaluation of Ad-BMP-2 for enhancing fracture healing in an infected defect fracture rabbit model." *J Orthop Res*, vol. 22, no. 1, pp. 66-72, 2004. View at: [Publisher Site](#) | [PubMed](#)